Molecular Biology of the Cell
Vol. 18, 3656–3666, September 2007

Endocytic Down-Regulation of ErbB2 Is Stimulated by Cleavage of Its C-Terminus[D] [V]

Mads Lerdrup,* Silas Bruun,* Michael V. Grandal, Kirstine Roepstorff, Malene M. Kristensen, Anette M. Hommelgaard, and Bo van Deurs

Department of Cellular and Molecular Medicine, University of Copenhagen, The Panum Institute, DK-2200 Copenhagen N, Denmark

Submitted January 12, 2007; Revised June 6, 2007; Accepted June 29, 2007
Monitoring Editor: Robert Parton

High ErbB2 levels are associated with cancer, and impaired endocytosis of ErbB2 could contribute to its overexpression. Therefore, knowledge about the mechanisms underlying endocytic down-regulation of ErbB2 is warranted. The C-terminus of ErbB2 can be cleaved after various stimuli, and after inhibition of HSP90 with geldanamycin this cleavage is accompanied by proteasome-dependent endocytosis of ErbB2. However, it is unknown whether C-terminal cleavage is linked to endocytosis. To study ErbB2 cleavage and endocytic trafficking, we fused yellow fluorescent protein (YFP) and cyan fluorescent protein (CFP) to the N- and C-terminus of ErbB2, respectively (YFP-ErbB2-CFP). After geldanamycin stimulation YFP-ErbB2-CFP became cleaved in nonapoptotic cells in a proteasome-dependent manner, and a markedly larger relative amount of cleaved YFP-ErbB2-CFP was observed in early endosomes than in the plasma membrane. Furthermore, cleavage took place at the plasma membrane, and cleaved ErbB2 was internalized and degraded far more efficiently than full-length ErbB2. Concordantly, a C-terminally truncated ErbB2 was also readily endocytosed and degraded in lysosomes compared with full-length ErbB2. Altogether, we suggest that geldanamycin leads to C-terminal cleavage of ErbB2, which releases the receptor from a retention mechanism and causes endocytosis and lysosomal degradation of ErbB2.

INTRODUCTION

The receptor tyrosine kinase ErbB2 is a potent oncoprotein, and a high ErbB2 level can by itself activate ErbB receptors (Worthylake *et al.,* 1999). Concordantly, increased ErbB2 levels can be found in several cancers (Klapper *et al.,* 2000; Yarden, 2001), and high ErbB2 levels are correlated to a worse prognosis for breast cancer patients (Slamon *et al.,* 1987; Hynes and Stern, 1994; De Placido *et al.,* 1998; Pegram *et al.,* 1998). Gene amplification is the most studied mechanisms causing high ErbB2 levels, but also posttranscriptional regulation of ErbB2 plays a role in cancers (Vernimmen *et al.,* 2003; Magnifico *et al.,* 2007). Little attention has been paid to the role of ErbB2 degradation in cancers, although when compromised it also would lead to increased ErbB2 levels and activity. Several studies have shown that endocytic down-regulation of ErbB2 is impaired in cancer cells (Sorkin *et al.,* 1993; Baulida *et al.,* 1996; Wang *et al.,* 1999; Hommelgaard *et al.,* 2004; Austin *et al.,* 2004; Longva *et al.,* 2005), and ErbB2 can even transmit this property to the related epidermal growth factor receptor (EGFR; Muthuswamy *et al.,* 1999; Wang *et al.,* 1999; Worthylake *et al.,* 1999; Haslekas *et al.,* 2005). Inhibition of HSP90 (e.g., with geldanamycin [GA]) leads to increased internalization and lysosomal degradation of ErbB2 in a manner depending on proteasomal activity (Tikhomirov and Carpenter, 2000; Austin *et al.,* 2004; Lerdrup *et al.,* 2006). HSP90 inhibition also induces cleavage of the cytoplasmic part of ErbB2, resulting in a transmembrane 135-kDa ErbB2 and short-lived cytoplasmic fragments (Tikhomirov and Carpenter, 2000; Lerdrup *et al.,* 2006). The cleavage occurs in the kinase domain and a similar cleavage is seen after stimulation with curcumin or staurosporine (Tikhomirov and Carpenter, 2001) or in cells with high levels of $\alpha 6\beta 1$ integrin (Shimizu *et al.,* 2003).

It has remained elusive whether endocytosis and C-terminal cleavage of ErbB2 are independent or correlated events. If positively correlated, C-terminal cleavage of ErbB2 could promote endocytosis by releasing ErbB2 from a retention mechanism that normally sequesters the receptor at the plasma membrane (Sorkin *et al.,* 1993; Hommelgaard *et al.,* 2004; Lerdrup *et al.,* 2006) or by exposure of an unknown cryptic motif stimulating endocytosis. In support of this, Tikhomirov and Carpenter (2003) observed that a C-terminally truncated mutant, ErbB2ΔC990, was destabilized. Alternatively, cleavage could occur as a consequence of endocytosis, e.g., in order to attenuate signaling from endosomes, as in insulin receptor signaling (Wiley and Burke, 2001). A similar mechanism was previously demonstrated for the Notch receptor that requires endocytosis for its intracellular cleavage (Gupta-Rossi *et al.,* 2004).

In the present study we have therefore asked whether C-terminal cleavage of ErbB2 stimulates endocytic down-regulation of ErbB2 or vice versa. We here report that a fluorescent ErbB2 fusion protein lacking the C-terminal tail similarly to ErbB2ΔC990 readily becomes internalized and degraded in lysosomes in unstimulated cells. Furthermore, Western blots of internalized ErbB2 and imaging of a full-length ErbB2 doubly tagged with fluorescent proteins con-

This article was published online ahead of print in *MBC in Press* (http://www.molbiolcell.org/cgi/doi/10.1091/mbc.E07–01–0025) on July 11, 2007.

[D] [V] The online version of this article contains supplemental material at *MBC Online* (http://www.molbiolcell.org).

* These authors contributed equally to this work.

Address correspondence to: Bo van Deurs (b.v.deurs@mai.ku.dk).

firmed that a larger relative amount of cleaved ErbB2 was present in the endocytic pathway than on the plasma membrane of GA-stimulated cells. Importantly, this ErbB2 cleavage took place already at the plasma membrane and depended on proteasomal activity. In GA-stimulated cells cleaved ErbB2 was degraded in lysosomes ~20-fold more efficiently than full-length ErbB2 because of increased internalization and reduced recycling. Altogether, this suggests that ErbB2 is normally retained from the endocytic machinery by its C-terminal tail and that C-terminal cleavage of ErbB2 releases it from this retention.

MATERIALS AND METHODS

Cell Culture

SK-BR-3, BT474, and HEp2 cells (American Type Culture Collection, Manassas, VA) were grown at 37°C, 5% CO_2 in DMEM supplemented with 10% FCS (Biochrom KG, Cambridge, United Kingdom), 2 mM glutamine, 200 U/ml penicillin, and 50 ng/ml streptomycin. BT474 cells were also supplemented with 5 μg/ml insulin. Except for DMEM, all reagents were obtained from Invitrogen (Carlsbad, CA).

Subcloning of Fluorescent ErbB2 Constructs

The YFP-ErbB2-CFP (YEC) was constructed using an ErbB2-CFP construct (Lerdrup *et al.*, 2006) and pEYFP-C1 (Clontech, Palo Alto, CA). Between ErbB2's signal sequence (amino acids: MIIME LAAWC RWGFL LALLP PGIA) and actual protein, we inserted the restriction sites ScaI and SalI in order to insert YFP. YFP-ErbB2 and YFP-ErbB2ΔC994 were PCR amplified from YEC using the primers GCTGGTTTAGTGAACCGTCAGATCC and GGTACCTCATACAGGTACATCCAGGCC or AAGCTTCTAGATGACCACAAAACGCTGGGGG, gel purified, and Topo-ligated into pcDNA3.1D/V5-His-TOPO. All constructs were sequenced to avoid unwanted mutations.

Biotin Internalization Assay

Cells were washed with ice-cold phosphate-buffered saline (PBS) and incubated twice with 0.5 mg/ml Sulfo-NHS-SS-Biotin (Pierce, Rockford, IL) for 20 min at 4°C. Next, cells were washed with ice-cold DMEM-HEPES plus 1% bovine serum albumin (BSA) for 10 min at 4°C, followed by incubation with DMEM-HEPES plus 0.2% BSA and 2 mM glutamine with 0.3, 1, 3, 10, or 30 μM GA (Sigma-Aldrich, St. Louis, MO) and when indicated also 500 nM bafilomycin A1 (Sigma-Aldrich), 10 μM monensin (Sigma-Aldrich), or 10 μM lactacystin (Sigma-Aldrich) for 2 h at 37°C. Control cells were incubated with DMEM-HEPES plus 0.2% BSA and 2 mM glutamine with 0.2 or 2% DMSO for 2 h at 4 or 37°C. Cells were transferred back onto ice and washed. Biotin on the plasma membrane was cleaved off using a reducing solution (50 mM 2-sodium-2-mercaptoethane-sulfonate (Sigma-Aldrich), 100 mM NaCl, 50 mM Tris-HCl, pH 8.7, 2.5 mM $CaCl_2$) for 20 min at 4°C three times. Cells were washed with ice-cold PBS, scraped off in lysis buffer (20 mM MOPS, 1 mM EDTA, pH 8, 150 mM NaCl, 3.5 mM SDS, 1% NP-40, 25 mM sodium deoxycholate (DOC), and phosphatase inhibitor cocktail 1:100; Sigma-Aldrich), sonicated, and centrifuged for 10 min at 16,000 × *g* at 4°C. Protein levels were determined and the samples were standardized. streptavidin-coated beads (Sigma-Aldrich) were added, and samples incubated overnight at 4°C. Samples were centrifuged for 1 min at 800 × *g* at 4°C, and the pellet washed in lysis buffer three times. The pellet was dissolved in lysis buffer with Laemmli buffer, 50 mM dithiothreitol was added, and the sample was subjected to Western blot analysis.

Western Blotting

The samples were subjected to SDS-PAGE using 6 or 8% acrylamide gels and transferred to a polyvinylidene fluoride (PVDF) membrane (Amersham Biosciences, Piscataway, NJ). Membranes were blocked with 5% milk powder (Bio-Rad, Richmond, CA) in PBS-0.1% Tween 20 followed by incubation with anti-ErbB2 (R&D Systems, Minneapolis, MN, AF1129) and afterward HRP-conjugated secondary antibodies (DAKO, Carpinteria, CA). Imaging and quantification of bands was done using ECL (Amersham Biosciences) and an AutoChemi system darkroom (UVP, San Gabriel, CA).

Microscopy

Cells plated on eight-well normal or coverslip chamber slices (Lab-Tek, Naperville, IL) were allowed to grow for 24 h and transfected (Fugene6, Roche, Indianapolis, IN) with ErbB2 constructs and/or TfR-GFP (Burack *et al.*, 2000), Rab7-GFP (Bucci *et al.*, 2000), Lamp1-GFP or CD63-GFP (kind gifts from Frederik Vilhardt, University of Copenhagen, Denmark) where indicated. Forty-eight hours after transfections (or plating for untransfected cells) cells were incubated with 3 μM GA, 10 μM lactacystin (Sigma-Aldrich), 500 nM bafilomycin A1 (Sigma-Aldrich), 10 μM monensin (Sigma-Aldrich), and/or 250 μM ALLN (calpain inhibitor I; Sigma-Aldrich) in culture medium for the indicated time at 37°C before fixation in 2% paraformaldehyde (PFA) or live cell imaging. Fixed cells were permeabilized and blocked in blocking buffer (5% goat serum with 0.2% saponin) for 20 min at room temperature (RT) and washed in PBS. Where indicated, cells were incubated with primary antibodies (mouse monoclonal Sc08 raised against the extracellular part of ErbB2, Santa Cruz Biotechnology, Santa Cruz, CA; rabbit polyclonal Ab-1 raised against aa. 1243–1255 of ErbB2, Neomarkers, Fremont, CA) in blocking buffer for 1 h at RT, washed, incubated with secondary antibody (Alexa-568– or Alexa-633–conjugated goat anti-mouse, Alexa-488 goat anti-rabbit, Invitrogen) in blocking buffer for 30 min at RT, washed, and mounted with Flouromount G (Southern Biotechnology Associates, Birmingham, AL).

For live cell imaging the medium was substituted with 37°C HEPES buffer (20 mM HEPES, pH 7.5, 140 mM NaCl, 2 mM $CaCl_2$, 10 mM KCl, 1 mg/ml glucose), and the cells were studied at 37°C using a heated microscope stage. All slides were examined with an LSM 510-Meta confocal microscope (Carl Zeiss, Thornwood, NY) equipped with 40× and 63× apochromat objectives. Cyan fluorescent protein (CFP), green fluorescent protein (GFP), and yellow fluorescent protein (YFP) were excited using a 458- or 488-nm Argon laser line, and their emissions were separated using hyperspectral imaging and linear unmixing with separately acquired reference spectra including a background spectrum. Alexa fluorophores were excited in multitrack-mode with the 488-nm Argon laser line, a 543-nm NeHe laser, or a 633-nm NeHe laser, and their emission was separated using conventional emission filtering. Images were processed (linear contrast enhancements and mild Gaussian blur to minimize noise) and quantitated using the LSM software v. 3.2 (Carl Zeiss) and WCIF compilation (http://www.uhnresearch.ca/facilities/wcif/imagej/) of ImageJ v1.37a (http://rsb.info.nih.gov/ij/).

Ratiometry Imaging and Color Coding of CFP and YFP Signals from YEC

The hyperspectral imaging and linear unmixing allowed us to simultaneously detect the overlapping CFP and YFP emissions with a fixed relative efficiency, allowing comparisons of YFP-CFP ratios between different samples with great reliability and without any influence from cell movements. Ratiometry images or movies were calculated and colored using a plugin we created for ImageJ, and the source code is available as Supplementary Videos, Textfile 1. Basically the software functioned on a pixel per pixel base by dividing the YFP channel with the CFP channel, applying a rainbow pseudocoloring (as seen in the color-coded bar in the figures), depending on the YFP-CFP ratio, and multiplying the intensity of this rainbow color with the average intensity of the CFP and YFP channels. The basic settings of the plugin were used for all ratiometry.

Pre-embedding Immunogold Labeling Electron Microscopy

SK-BR-3 cells were fixed in 0.1% glutaraldehyde and 2% formaldehyde in 0.1 M phosphate buffer at RT for 30 min. After a wash the cells were incubated with a rabbit polyclonal anti-GFP antibody (Molecular Probes, Eugene, OR; A11122) followed by protein A-gold (10 nm; Dr. G. Posthuma, University Medical Center, Utrecht). Then the cells were briefly fixed and incubated with free protein A, followed by unspecific rabbit IgG, and fixed again. After a wash the cells were next incubated with mouse monoclonal Sc08 (Santa Cruz Biotechnology) against the extracellular (N-terminal) part of ErbB2, followed by 5-nm gold–labeled goat anti-mouse antibody (Amersham Biosciences). After a brief fixation and a wash the cells were scraped off and further processed for Epon embedding and electron microscopy (pre-embedding immunogold labeling electron microscopy) as previously described (Hommelgaard *et al.*, 2004).

RESULTS

C-terminally Truncated ErbB2 Is Readily Endocytosed

To investigate whether C-terminal cleavage of ErbB2 promotes internalization of the receptor, we generated a deletion mutant similar to the metabolically unstable ErbB2ΔC990 described by Tikhomirov and Carpenter (2003). This mutant had YFP added N-terminally and was derived from rat ErbB2, allowing us to separately visualize localization of YFP-ErbB2ΔC994 (position 994 of rat ErbB2 corresponds to 990 of human ErbB2) and endogenous ErbB2 labeled with an antibody specific for human ErbB2. To ensure correct localization to the endoplasmic reticulum during translation and correct insertion into the membrane, YFP was added between the predicted signal sequence cleavage site of ErbB2 and the actual ErbB2 protein (Bendtsen *et al.*, 2004). In unstimulated SK-BR-3 breast cancer cells transfected with YFP-ErbB2ΔC994, a relatively large fraction of this protein was localized in cytoplasmic vesicles (Figure 1B), and in cells treated with bafilomycin for 2 h an even

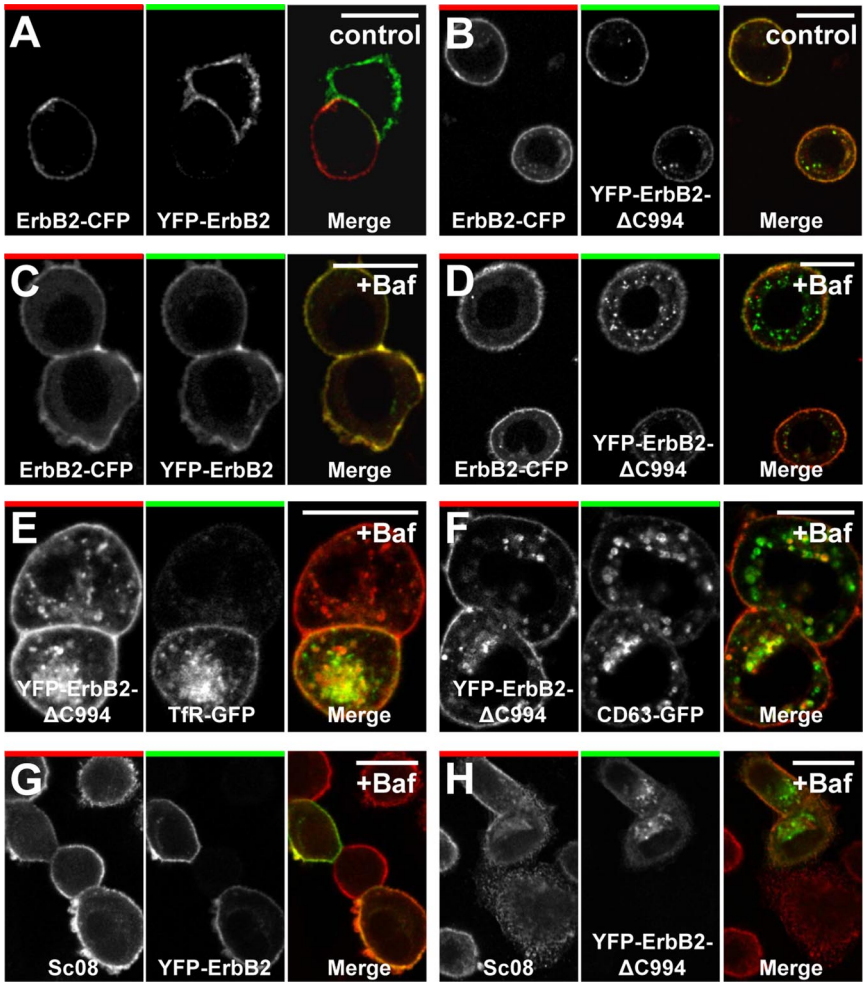

Figure 1. C-terminally truncated ErbB2 is readily internalized. (A and B) Confocal microscopy images of fixed SK-BR-3 cells transfected with ErbB2-CFP together with YFP-ErbB2 (A) or YFP-ErbB2ΔC994 (B) constructs based on rat ErbB2. (A and B) Left, CFP distribution; middle, YFP distribution; right, the merged signal (CFP, red; YFP, green). In contrast to full-length ErbB2 the truncated version becomes internalized to a detectable level. (C and D) Images similar to the ones in A and B, but cells were incubated with 500 nM bafilomycin for 2 h. Note the increased accumulation of truncated ErbB2-containing endocytic vesicles. (E and F) Confocal images of fixed SK-BR-3 cells transfected with YFP-ErbB2ΔC994 and TfR-GFP (E) or CD63-GFP (F) and incubated with 500 nM bafilomycin for 2 h. Truncated, internalized ErbB2 colocalizes with both markers. (G and H) Confocal microscopy images of fixed, bafilomycin-treated (500 nM) SK-BR-3 cells showing endogenous (human) ErbB2 labeled with Sc08 against ErbB2's N-terminal part together with transfected YFP-ErbB2 (G) or YFP-ErbB2ΔC994 (H). It is seen that endocytosis and vesicular accumulation after bafilomycin treatment is much higher for YFP-ErbB2ΔC994 than for YFP-ErbB2 and that YFP-ErbB2ΔC994 is present in endosomal and lysosomal compartments. Bars, 20 μm.

larger fraction was localized in cytoplasmic vesicles, suggesting that YFP-ErbB2ΔC994 is readily internalized and degraded in lysosomes (Figure 1D).

In contrast, very little cotransfected ErbB2-CFP (rat ErbB2 with a C-terminal CFP tag) or YFP-ErbB2 (rat) accumulated intracellularly regardless of bafilomycin treatment (Figure 1, A–D). To confirm that the intracellular compartments containing accumulated YFP-ErbB2ΔC994 actually were parts of the endosomal/lysosomal pathway, we coexpressed YFP-ErbB2ΔC994 with various markers of endocytic compartments fused to GFP. Indeed in bafilomycin-treated cells, YFP-ErbB2ΔC994 did accumulate in compartments positive for TfR-GFP, Rab7-GFP, CD63-GFP, or Lamp1-GFP (Figure 1, E and F, and data not shown). Immunostaining of endogenous ErbB2 confirmed that YFP-ErbB2, in contrast to YFP-ErbB2ΔC994, primarily colocalized with endogenous ErbB2 on the plasma membrane (Figure 1, G and H). The same was observed when colocalization was quantitated from a large number of cells (Supplementary Figure 1). To confirm that intracellular YFP-ErbB2ΔC994 did origin from the plasma membrane, we studied cells that have been pretreated with the protein synthesis inhibitor cycloheximide (CHX). After bafilomycin stimulation of these cells, a markedly higher accumulation of YFP-ErbB2ΔC994 than YFP-ErbB2 could be observed. When the fluorescence in the interior of cells treated this way was removed using photobleaching, subsequent time-lapse microscopy demonstrated a significant recovery of intracellular YFP-ErbB2ΔC994 fluorescence within 25 min. Given that these cells had their protein synthesis inhibited, this intracellular fluorescence has to originate from the surface (Supplementary Figure 1). Thus, the C-terminal truncation (ΔC994) of ErbB2, previously reported to destabilize ErbB2 (Tikhomirov and Carpenter, 2003), appears to promote internalization of the receptor.

Endocytosis Correlates Positively to Cleavage of ErbB2

To further investigate if C-terminal cleavage of ErbB2 and endocytosis are positively correlated, we stimulated SK-BR-3 cells with GA and used a biotin internalization assay to compare the size of internalized ErbB2 to that of ErbB2 in total cell lysates (Figure 2A). Using an antibody against the extracellular part of ErbB2, we observed both the full-length 185-kDa ErbB2 and cleaved 135-kDa ErbB2 lacking its C-terminal, cytoplasmic tail in total cell lysates (Figure 2A, top). A range of GA concentrations stimulated both internalization and cleavage of ErbB2 as previously described (Figure 2, A and B; Mimnaugh *et al.*, 1996; Tikhomirov and Carpenter, 2000, 2001, 2003; Austin *et al.*, 2004; Lerdrup *et al.*, 2006). Whereas virtually no ErbB2 was cleaved in control cells (Figure 2A, top), 25–70% of ErbB2 was cleaved in GA-stimulated cells (Figure 2A, top), and a very large fraction of the internalized ErbB2 (80–95% depending on GA concentration) was cleaved (Figure 2, A and B, bottom). Importantly, the ratio of cleaved to full-length ErbB2 was markedly higher in the internalized fraction compared with whole cell lysates at all GA concentrations (Figure 2A). This

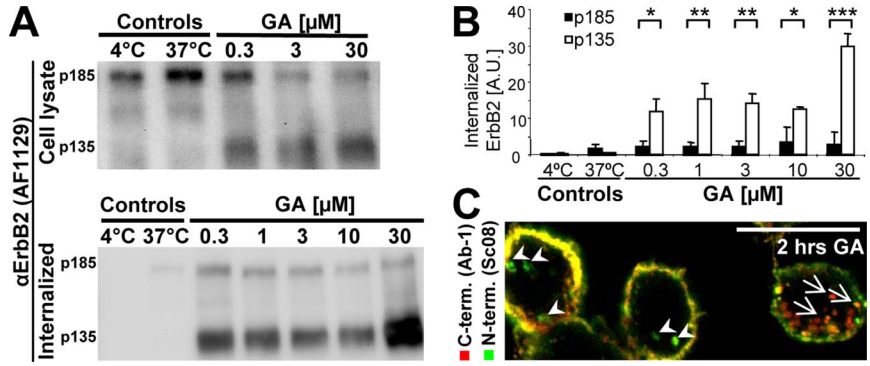

Figure 2. In GA-stimulated cells ErbB2 is preferentially internalized in a cleaved form. (A) Bottom, Western blot from a biotin internalization assay showing internalized full-length and cleaved ErbB2 (p185 and p135, respectively) in SK-BR-3 cells incubated for 2 h with geldanamycin (GA) at the indicated concentrations. Control cells were incubated with the highest DMSO concentration presented to GA-incubated cells. Top, Western blot of full-length and cleaved ErbB2 in the whole cell lysates from which the biotinylated ErbB2 was precipitated. (B) Quantification of internalized ErbB2 measured in arbitrary units (AU) from Western blots like the one in A; n = 3, error bars, SD; *p < 0.05, **p < 0.01, ***p < 0.001, in a two-sided Student's *t* test. (C) Confocal image of SK-BR-3 cells incubated with 3 μM GA for 2 h and then stained for N- and C-terminal, endogenous ErbB2 (Sc08, green, and Ab-1, red, respectively). Arrows and arrowheads point at structures with predominant C- and N-terminal staining, respectively. Bar, 20 μm.

demonstrates a positive correlation between endocytosis and cleavage of ErbB2, but not whether cleavage promotes endocytosis or vice versa. To confirm the difference in cleavage between endocytosed and plasma membrane ErbB2 in GA stimulated cells by an independent method, we performed immunofluorescence and confocal microscopy of GA-stimulated cells. In concordance with the biotin internalization assay, when compared with the plasma membrane, vesicular structures had a stronger labeling of the extracellular part of ErbB2 relative to the intracellular part (Figure 2C, arrowheads). However, we could also observe vesicular structures with a strong labeling of the intracellular part of ErbB2 relative to the extracellular part (Figure 2C, arrows).

YEC Allows Ratiometric Imaging of ErbB2 Cleavage

Immunofluorescence is sensitive to varying and inefficient labeling, i.e., due to epitope-concealment in some compartments, rendering it an ill-suited method for ratiometric measurements. To study the role of cleavage for ErbB2 endocytosis in further details, we needed a more reliable and reproducible quantification of the ratio between the extracellular and intracellular parts of ErbB2 on the plasma membrane and in the various endocytic compartments. We therefore constructed a doubly tagged fluorescent fusion protein comprising YFP fused to rat ErbB2's N-terminus and CFP fused its C-terminus (YEC); Figure 3A). By using rat ErbB2 for construction of YEC, we were able to track endogenous ErbB2 selectively with an antibody specific for human ErbB2. Live cell imaging of SK-BR-3 cells expressing YEC revealed YFP and CFP fluorescence colocalized primarily to the plasma membrane. To verify that YEC at the plasma membrane had the correct topology, living cells were trypsinized in situ during imaging (Figure 3B). Although trypsinized cells rounded up due to perturbed adhesion within a few minutes, it was clear that YFP fluorescence quickly vanished. In contrast, CFP was untouched by trypsin, confirming that it was located intracellularly (Figure 3B). By immunogold labeling and electron microscopy of the surface of intact, fixed cells, it was evident that YEC and endogenous ErbB2 colocalized to a high degree and primarily on plasma membrane protrusions (Figure 3E). We could furthermore confirm that overexpressed YEC behaved similar to overexpressed wild-type rat ErbB2 in respect to basal and GA-induced degradation as well as EGF-induced phosphorylation (Supplementary Figure 2).

Immunofluorescence of endogenous ErbB2 and YEC in SK-BR-3 cells after GA stimulation revealed that ErbB2 and YEC colocalized in vesicular compartments, confirming that YEC behaves like endogenous ErbB2 (Figure 3C). It was recently reported that EGFR was cleaved intracellularly in apoptotic cells (He *et al.*, 2006). Similarly, spontaneously apoptotic cells expressing YEC clearly lacked colocalization between YFP and CFP, indicating that ErbB2 is also cleaved in apoptotic cells. In contrast, nonapoptotic cells had a clear colocalization of YFP and CFP at the plasma membrane (Figure 3D). To facilitate the interpretation of the YEC signal, YFP fluorescence was divided by CFP fluorescence pixel by pixel, yielding a ratiometric image useful for evaluating the amount of cleavage. The YFP-CFP ratio is based on arbitrary fluorescence intensities; thus a ratio of 1.0 does not correspond to a 1:1 M ratio between YFP and CFP. All ratiometric images shown here are rainbow color–coded according to the YFP-CFP ratio, and the intensity of the ratio image is controlled by the intensity of the average YFP+CFP signal in each pixel (Figure 3D).

Endocytosed ErbB2 Is Cleaved

To confirm the positive correlation between cleaved and endocytosed ErbB2 seen with the biotin internalization assay, we used confocal microscopy to track YEC localization and cleavage in SK-BR-3 cells after GA stimulation. In fixed and permeabilized cells cleavage of the intracellular part of ErbB2 was visible both at the plasma membrane and in vesicular structures after GA stimulation (Figure 4A, seen as an increase in YFP-CFP ratio). Importantly, most vesicles had a higher YFP-CFP ratio than the plasma membrane (Figure 4A, arrowheads), but we could also observe vesicles with a markedly lower YFP-CFP ratio (Figure 4A, arrows). Similar results were found with BT474 breast cancer cells and with SK-BR-3 cells expressing a variant of YEC that was based on human ErbB2 (data not shown). Quantification of the YFP-CFP ratio in vesicles and at the plasma membrane of individual SK-BR-3 cells demonstrated that in most cells, the average YFP-CFP ratio was higher in vesicles compared with the plasma membrane (Figure 4B).

ErbB2 cleavage could either occur at the plasma membrane or en route to lysosomes. To clarify the YEC cleavage status in endosomes and lysosomes, we coexpressed YEC with various markers of these compartments, i.e., TfR-GFP, Rab7-GFP, Lamp1-GFP, or CD63-GFP. After 2 h of GA stimulation, much YEC colocalized with lysosomal markers, such as Lamp1-GFP and CD63-GFP (Figure 4, C and D). YEC was extensively cleaved in most lysosomes (Figure 4, C and D, yellow and red structures), but a few late endosomes/lysosomes also contained a high amount of CFP compared

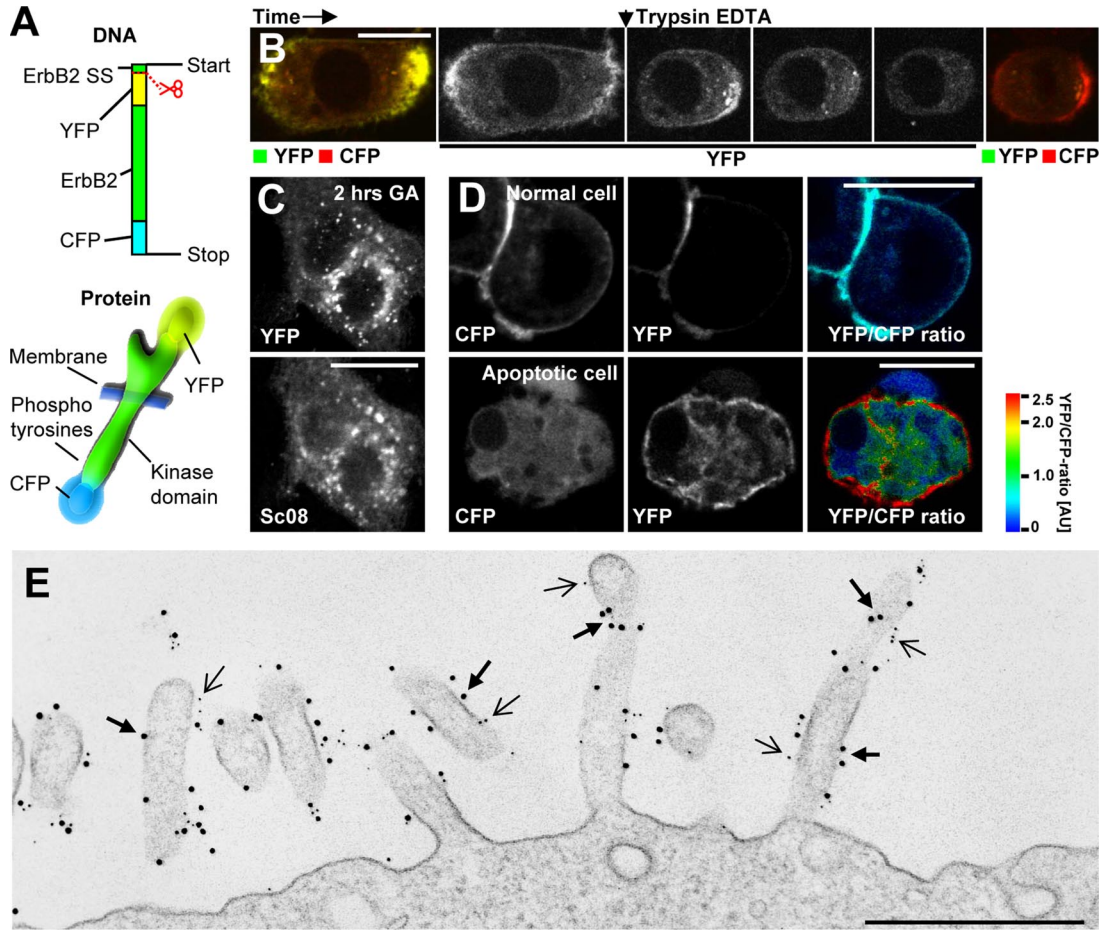

Figure 3. Validation of YEC. (A) Structure of YEC at the DNA and protein levels. This construct is based on rat ErbB2. The scissor indicates the cleavage after the signal sequence (SS). (B) Time-lapse, live cell, confocal microscopy of SK-BR-3 cells transfected with YEC showing the effect of trypsin on YEC. Left image, the localization and intensity of YFP and CFP before incubation with 0.05% trypsin (yellow indicates colocalization). Middle images, the change in YFP intensity (extracellular) only. Right image, the localization and intensity of YFP and CFP after few minutes of trypsin incubation. It is seen that the YFP-tagged, N-terminal part of YEC is indeed extracellular and therefore sensitive to trypsin. (C) Confocal microscopy images showing the localization of YEC (YFP, top) or endogenous ErbB2 (Sc08, bottom) in the same YEC-transfected, fixed SK-BR-3 cell after 2 h of GA incubation. YEC clearly colocalizes with endogenous ErbB2. (D) Live cell confocal microscopy of SK-BR-3 cells transfected with YEC. Left images, the localization of CFP; middle, the localization of YFP; and right, the ratio between YFP and CFP as explained in the color bar. Red, a high YFP-CFP ratio; blue, a low YFP-CFP ratio. Please note that the YFP-CFP ratio is based on arbitrary fluorescence intensities and that a ratio of 1.0 does not correspond to a 1:1 molar ratio between YFP and CFP. The intensity of each pixel in the image is encoded by average YFP and CFP fluorescence. Top, a normal SK-BR-3 cell; bottom, an apoptotic cell. (E) Electron microscopy image of an immunogold-labeled SK-BR-3 cell transfected with YEC. Gold particles, 10-nm, mark YFP (thick arrows); 5-nm gold particles mark endogenous ErbB2 (thin arrows). Bars, (B–D) 20 μm; (E) 500 nm.

with YFP (Figure 4, C and D, blue structures). Importantly, in cells coexpressing the endosomal marker TfR-GFP most YEC in TfR-GFP–positive endosomes was cleaved (Figure 4E, red and yellow structures), suggesting that cleavage of the intracellular part of ErbB2 was not a result of proteolysis along the endosomal/lysosomal degradation pathway. To confirm this finding, we performed live cell 4D (3D over time) confocal microscopy of YEC in GA-stimulated SK-BR-3 cells. This showed that newly formed vesicles had a high YFP-CFP ratio already at their first appearance, supporting that ErbB2 is cleaved before internalization (Figure 4F; Supplementary Movie 1). When following these vesicles, a sudden reduction in the YFP-CFP ratio was visible after a few minutes because of acidification of the vesicular lumens containing the YFP-tagged part of YEC (Figure 4, Supplementary Figure 2). Altogether this supports that YEC is cleaved before it enters the more acidic lysosomes.

GA-induced Cleavage of ErbB2 at the Plasma Membrane Increases Its Lysosomal Degradation

In agreement with ErbB2 being cleaved before internalization, many cells had increased YFP-CFP ratios at the plasma membrane after GA stimulation (examples in Figure 5A). To strengthen this finding, we measured plasma membrane YFP-CFP ratios of a large number of cells with and without GA stimulation. The majority of unstimulated cells had a plasma membrane YFP-CFP ratio of approximately 0.25, and a few unstimulated cells had a YFP-CFP ratio larger than 1.0. Cells stimulated with GA for 2 h had more heterogeneous and significantly higher YFP-CFP ratios at the plasma membrane than unstimulated cells ($p \ll 0.001$, Mann-Whitney two-tailed U test; Figure 5B), suggesting that cleavage of the intracellular part of ErbB2 occurs before its internalization. This increased cleavage of plasma membrane ErbB2 was not due to apoptosis (Supplementary Figures 3 and 4). The

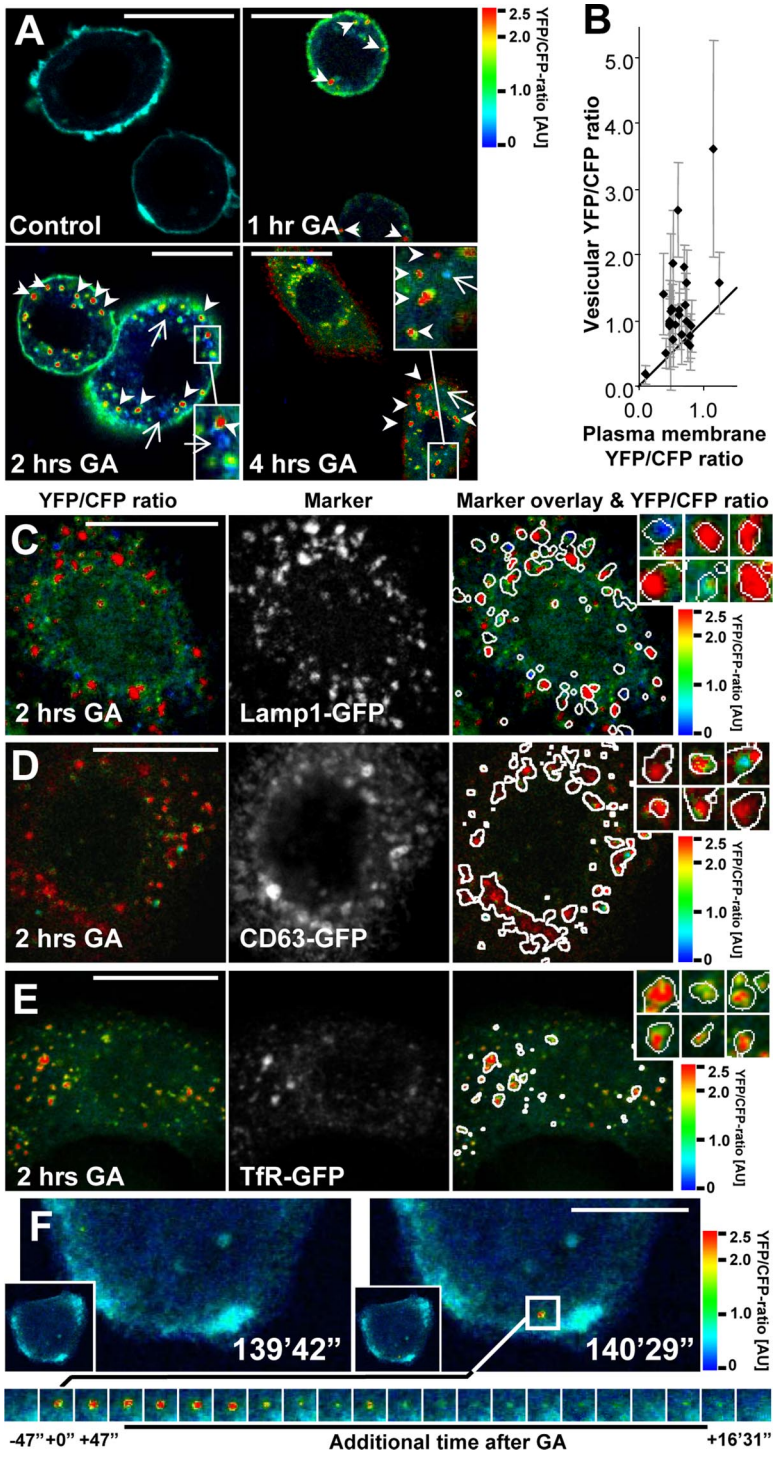

Figure 4. YEC in endocytic compartments shows a high YFP-CFP ratio. (A) Ratio images of YFP-CFP in YEC expressing SK-BR-3 cells after 0–4 h of 3 μM GA treatment followed by fixation and permeabilization. Arrows and arrowheads point at vesicles with predominant CFP (blue) or YFP (red) staining, respectively. (B) Quantification of plasma membrane versus vesicular YFP-CFP-ratios. Each dot is a cell; error bars, SD. (C–E) Confocal images of fixed SK-BR-3 cells transfected with YEC and GFP-tagged markers for endosomes or lysosomes after 2 h of 3 μM GA treatment. Left images, the YFP-CFP ratio. Middle images, the intracellular marker localization (Lamp1-GFP, CD63-GFP, and TfR-GFP in C–E, respectively). Right images, the ratio images with an overlay of the intracellular marker localization shown as white circumferences. Inserted images, enlargements of YEC and marker positive vesicles. It is seen that Lamp1-GFP, CD63-GFP, and TfR-GFP–containing vesicles generally have a high YFP-CFP ratio. (F) Live cell 4D ratio imaging of a GA-stimulated SK-BR-3 cell. Left image, the cell 139 min and 42 s after incubation with 3 μM GA and just before the formation of a vesicle with high YFP-CFP ratio. Right images, the cell just after formation of the vesicle. The bottom panel of images tracks the fate of the vesicle in the following 16 min and 31 s. It is seen that the vesicle initially has a high YFP-CFP ratio that is reduced after some time because of acidification. Bars, 20 μm.

increase in the YFP-CFP ratio of plasma membrane YEC after GA stimulation could be due to ErbB2 cleavage in the endocytic pathway and recycling of cleaved ErbB2 to the plasma membrane. However this can be ruled out, because inhibition of recycling with monensin did not reduce the cleavage of YEC at the plasma membrane significantly ($p = 0.38$, Mann-Whitney two-tailed U test), demonstrating that cleavage of the intracellular part of ErbB2 actually does take place at the plasma membrane (Figure 5, D and E). Disruption of the actin cytoskeleton with latrunculin reduced endocytosis of YEC, and most intracellular YEC was in the biosynthetic pathway. However, YEC was still efficiently cleaved at the plasma membrane in latrunculin-treated cells having little endocytosis, confirming that ErbB2 is cleaved at the plasma membrane (Figure 5F).

Next, we wanted to investigate to what extent cleavage regulated ErbB2 trafficking. Although recycling is not needed for the presence of cleaved ErbB2 at the plasma membrane, both full-length p185 and cleaved p135 ErbB2 did recycle in GA-stimulated cells. Monensin treatment led

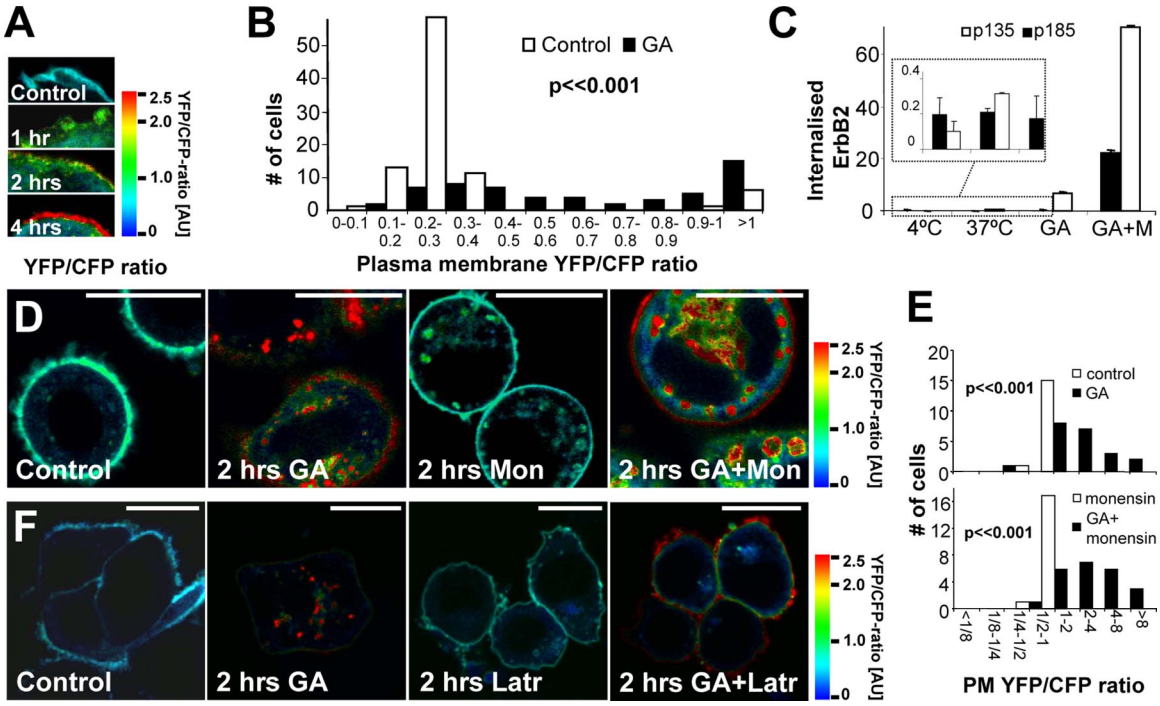

Figure 5. ErbB2 cleavage occurs at the plasma membrane and is not due to recycling from the endocytic pathway. (A) Ratio images of the plasma membrane of fixed, YEC-transfected SK-BR-3 cells treated with 3 μM GA for 0–4 h. (B) Quantitative ratiometry of individual cell membranes from living YEC-transfected SK-BR-3 cells. □, untreated controls; ■, GA-treated cells (2 h). Column height represents the number of cells with the particular ratios. Data were tested with a two-sided Mann-Whitney U test. (C) Biotin internalization assay showing the effect of 10 μM monensin (M) on the 3 μM GA-induced internalized pool of full-length and cleaved ErbB2 after 2 h. Insert, the relatively low values of the first five samples are shown with a scaled-up Y-axis. It is seen that monensin causes a marked increase in intracellular ErbB2 after GA stimulation, and the relative increase for GA+M compared with GA only samples is highest for full-length ErbB2, suggesting that it recycles more efficiently than cleaved ErbB2. Error bars, SD. (D) Ratio images of fixed YEC-transfected SK-BR-3 cells incubated with 3 μM GA and/or 10 μM monensin for 2 h or left as control. Note that YEC is still cleaved at the plasma membrane after GA stimulation when recycling is inhibited with monensin. (E) Distribution of the YFP-CFP ratio on the plasma membrane (PM) of cells treated as in D. Data were tested with two-sided Mann-Whitney U tests. (F) Ratio images of fixed YEC-transfected SK-BR-3 cells incubated with 20 μg/ml latrunculin A and/or 3 μM GA for 2 h or left as control. Note that YEC is still cleaved at the plasma membrane although latrunculin inhibits accumulation of intracellular YEC after GA stimulation. Bars, 20 μm.

to a more than 10-fold increase in biotinylated, internalized p135 ErbB2 (Figure 5C), whereas internalized p185 ErbB2 accumulated 133-fold (Figure 5C). This suggests that a relatively larger fraction of internalized cleaved ErbB2 is targeted for degradation in lysosomes compared with full-length ErbB2. To investigate this further, GA-stimulated cells were incubated with or without bafilomycin that inhibits lysosomal acidification and activity (van Deurs *et al.*, 1996). When lysosomal degradation was inhibited, the biotin internalization assay showed a fourfold increase in internalized p135 ErbB2 but no effect on p185 ErbB2 in GA-stimulated cells (Figure 6A). Bafilomycin caused a profound accumulation of cleaved YEC in vesicular structures in most GA-stimulated cells, whereas YEC was extensively degraded in the majority of cells stimulated with GA alone for 4 h (Figure 6B). It is striking that in cells costimulated with bafilomycin and GA the amount of p135 ErbB2 accumulating was 20-fold higher than that of p185 ErbB2 (Figure 6A), demonstrating that cleavage not only markedly increases the probability of ErbB2 being internalized, but also its rate of lysosomal degradation.

Cleavage of ErbB2 Depends on Proteasomal Activity

We have previously demonstrated that GA-induced internalization of ErbB2 depends on proteasomal activity (Lerdrup *et al.*, 2006). Because we found that cleavage of ErbB2 promotes its endocytosis, we also investigated whether the requirement of proteasomal activity was an upstream or downstream event of cleavage. First, we could demonstrate that the proteasome inhibitor lactacystin inhibited internalization of cleaved p135 ErbB2 efficiently (Figure 7A). This could either be because ErbB2 cleavage at the plasma membrane is reduced, leading to reduced ErbB2 internalization, or because ErbB2 internalization itself was inhibited. To distinguish between these two possibilities, we investigated whether inhibition of the proteasome affected cleavage of ErbB2 at the plasma membrane. GA-stimulated, YEC-expressing cells were cotreated with one of the proteasomal inhibitors, lactacystin or ALLN. Both inhibitors completely abolished the GA-induced cleavage of plasma membrane–located YEC, suggesting that proteasomal activity is a requirement for GA-induced cleavage of ErbB2 (Figure 7, B and C). If proteasomal activity is an upstream event of ErbB2 cleavage, then it is likely that the proteasomal activity required for ErbB2 internalization after GA stimulation is needed for ErbB2 cleavage rather than the internalization itself. To see if this was the case, we treated cells coexpressing YFP-ErbB2ΔC994 and ErbB2-CFP with lactacystin and compared them to unstimulated cells. YFP-ErbB2ΔC994 was readily internalized in both unstimulated and lactacystin-stimulated cells (Figure 7D), showing that internalization of truncated ErbB2 occurred independently of proteasomal activity. Altogether this suggests that proteasomal activity is an upstream regulator of ErbB2

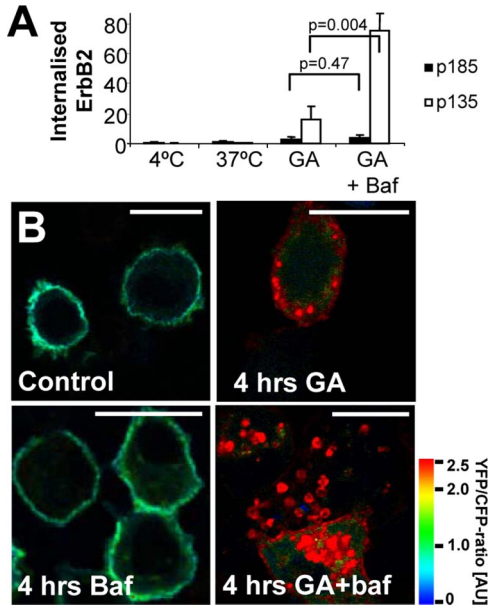

Figure 6. Cleavage of ErbB2 increases its lysosomal targeting. (A) Biotin internalization assay showing the effect of 500 nM bafilomycin (baf) on the 3 μM GA-induced internalized pool of full-length and cleaved ErbB2 after 2 h. Data were tested with two-sided Student's *t* tests. Error bars, SD. (B) Ratio images of fixed, YEC-transfected SK-BR-3 cells incubated with 3 μM GA and/or 500 nM bafilomycin for 4 h or left as control. It is seen that much cleaved but little full-length ErbB2 accumulate intracellularly after GA stimulation if lysosomal degradation is inhibited. Bars, 20 μm.

cleavage after GA stimulation and that proteasomal activity is not needed for the internalization of ErbB2 once it is cleaved.

DISCUSSION

We here show that endocytic down-regulation of ErbB2 is promoted by cleavage of its C-terminus. A YFP-tagged C-terminal deletion mutant of ErbB2, YFP-ErbB2ΔC994, was internalized and degraded in lysosomes far more efficiently than full-length ErbB2 in unstimulated cells. Using biochemical methods, advanced microscopy, and the doubly fluorescent fusion protein YEC, we demonstrated a clear link between cleavage and endocytosis of ErbB2 in GA-stimulated cells. We furthermore showed that cleavage happens at the plasma membrane in a proteasome-dependent manner before the induced internalization and subsequent lysosomal degradation of ErbB2. After GA stimulation, cleaved ErbB2 recycled to a smaller degree and was degraded in lysosomes as much as 20-fold more efficiently than full-length ErbB2.

Several central conclusions of the present article were aided and strengthened by the use of the reporter construct YEC, which we have shown is a reliable and efficient tool to obtain spatiotemporal information about ErbB2 cleavage in single cells and subcellular compartments. We envision that such a construct can also be used for live cell studies of shedding of the extracellular part of ErbB2 and the consequences of shedding for ErbB2 function, localization, and mobility. Furthermore, it could even be used for studies of ErbB2 cleavage in transgene animals. Cleavage is also an important regulator of other proteins, e.g., ErbB4, Met, Notch, CD44, p75/NTR, and APP (Selkoe *et al.*, 1996; Haass and De, 1999; Wallenius *et al.*, 2000; Ni *et al.*, 2001; Zampieri *et al.*, 2005; Petrelli *et al.*, 2006; Sugahara *et al.*, 2006), and tandem fusion proteins made from these proteins similarly to YEC could be highly useful. An important advantage of such constructs is that one avoids the problems inherent to ratiometric studies based on immunofluorescence, namely availability of protein epitopes and steric hindrance. Indeed, doubly fluorescent reporter proteins are not failure-free, and they should be supplemented by other methods. In the present study the major findings obtained with YEC are in agreement with data obtained by a biotin internalization assay.

ErbB2 Is Cleaved at the Plasma Membrane

The GA-induced cleavage of ErbB2, which has previously been observed in Western blots (Tikhomirov and Carpenter, 2000, 2001, 2003), could essentially be a result of proteolysis of internalized ErbB2 in the endosomal/lysosomal degrada-

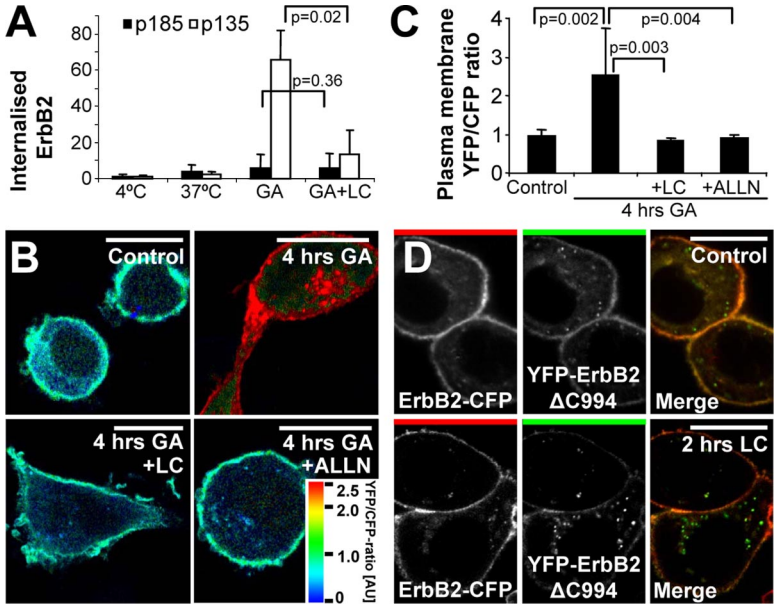

Figure 7. GA-induced cleavage of ErbB2 depends on proteasomal activity. (A) Biotin internalization assay showing the effect of 10 μM of the proteasomal inhibitor lactacystin (LC) on the 3 μM GA-induced internalized pool of full-length and cleaved ErbB2 after 2 h. Data were tested with two-sided Student's *t* tests. Error bars, SD. (B) Ratio images of YEC-transfected, fixed SK-BR-3 cells incubated with 3 μM GA and when indicated also 10 μM lactacystin or 250 μM of the broad protease inhibitor ALLN for 4 h or left as control. (C) Distribution of the YFP-CFP ratio on the plasma membrane of cells treated as in B. Data were tested with two-sided Mann-Whitney U tests. Error bars, 95% confidence intervals. (D) Confocal microscopy images of fixed SK-BR-3 cells cotransfected with ErbB2-CFP and YFP-ErbB2ΔC994 and either treated with 3 μM lactacystin for 2 h or left untreated. It is seen that cleavage and internalization of full-length ErbB2 depends on proteasomal activity and that YFP-ErbB2ΔC994 is internalized even when proteasomal activity is inhibited. Bars, 20 μm.

tion pathway. Here we demonstrate by several means that ErbB2 is cleaved at the plasma membrane. First, ratiometry demonstrated that YEC localized to the plasma membrane is cleaved after GA stimulation. Second, ErbB2 was already cleaved in early endosomes, ruling out cleavage en route in the lysosomal degradation pathway. Third, imaging of YEC in monensin- or latrunculin-treated cells confirmed that GA did induce YEC cleavage despite inhibited recycling or endocytosis.

Cleavage of ErbB2 Increases Its Internalization and Lysosomal Degradation

The biotin internalization assay investigating GA-stimulated ErbB2 internalization and cleavage demonstrated a clear difference in the behavior of full-length and C-terminally cleaved ErbB2. Most importantly, cells with inhibited lysosomal degradation accumulated 20-fold more cleaved p135 ErbB2 than full-length p185 ErbB2. This reflects the overall impact of cleavage on the rates of internalization and lysosomal targeting. We have demonstrated that the internalization of ErbB2 increases several fold after cleavage, and in most cells the YFP-CFP ratio of YEC in vesicles was higher than that of the plasma membrane YEC. Thus, a major factor contributing to the relatively high lysosomal degradation rate of p135 compared with p185 is an increased internalization rate. This conclusion is supported by the modest increase in the amount of internalized p185 ErbB2 after GA stimulation. Both p135 and p185 ErbB2 are recycled in GA-stimulated cells, but monensin treatment caused a 10-fold increase in intracellularly accumulated p135 ErbB2, whereas the relative effect on p185 ErbB2 was far higher. Altogether, this suggests that in GA-stimulated cells p185 is efficiently recycled and that cleavage increased the amount of ErbB2 targeted for lysosomal degradation.

We previously found that cleavage is not a requirement for ErbB2 internalization (Lerdrup *et al.*, 2006), and in agreement with this we here observed internalization of full-length ErbB2 after GA stimulation. However on the basis of immunofluorescence colocalization studies of the termini of ErbB2, we also observed an apparent inverse relationship between the amount of internalization and cleavage in each cell (Lerdrup *et al.*, 2006). A likely explanation of this is that we studied apoptotic as well as nonapoptotic cells and that apoptotic cells both had a reduced internalization and a sudden accumulation of cytoplasmic ErbB2 fragments that markedly reduced colocalization of ErbB2's termini (Supplementary Figures 3 and 4). In contrast, the more slow and moderate cleavage of ErbB2 in nonapoptotic, GA-stimulated cells studied here led to a less pronounced accumulation of cytoplasmic fragments and hence a smaller decrease in colocalization (Supplementary Figures 3 and 4). Lastly, the antibody used here reflects the amount of cleavage of the intracellular part of ErbB2 more accurately than the antibody cocktail used previously (Lerdrup *et al.*, 2006; Supplementary Figure 5).

Proteasomal Activity Is Needed for Cleavage of ErbB2

GA-induced degradation of ErbB2 can be inhibited by proteasomal inhibitors (Mimnaugh *et al.*, 1996), and a straightforward interpretation of this is that ErbB2 is degraded by the proteasome itself (Hong *et al.*, 1999; Zheng *et al.*, 2000; Xu *et al.*, 2001; Citri *et al.*, 2002; Way *et al.*, 2004). We recently demonstrated that proteasomal activity is needed for GA-induced internalization and lysosomal degradation of ErbB2 (Lerdrup *et al.*, 2006). Because we here show that cleavage of ErbB2 promotes its internalization, we asked if the cleavage of the intracellular part of ErbB2 also depended on proteasomal activity. In cells cotreated with GA and one of two proteasomal inhibitors, the GA-induced cleavage of ErbB2 was absent. These observations are in accordance with previous experiments (Tikhomirov and Carpenter, 2000). Interestingly, YFP-ErbB2ΔC994 was internalized regardless of inhibition of the proteasome. This suggests that the proteasomal dependence is at the cleavage step and that internalization of ErbB2 once it is cleaved is a proteasome independent process. The cleavage of ErbB2 after GA stimulation is due to endoproteolytic activity, giving rise to cytoplasmic fragments with short half-lives and a transmembrane p135 fragment that has a well-defined size, suggesting that the proteolysis occurs at a specific site (Tikhomirov and Carpenter, 2000, 2001, 2003). The simplest interpretation of the dependence of ErbB2 cleavage on proteasomal activity is that the proteasome is cleaving ErbB2 itself, although it would imply that the proteasome is able to cleave ErbB2 endoproteolytically. Interestingly, it was recently reported that the 20S proteasome actually functions as an endoprotease in processing of the NFκB precursor, p105 (Moorthy *et al.*, 2006). The requirement of proteasomal activity for ErbB2 cleavage could also be indirect. One possibility is that free ubiquitin becomes sequestered when the proteasome is inhibited with lactacystin. However, inhibition of proteasomal activity leads to an accumulation of ubiquitinylated ErbB2 (Zhou *et al.*, 2003; our unpublished data), and more importantly ErbB2 was found still to become ubiquitinylated in cells treated with lactacystin and GA (Mimnaugh *et al.*, 1996; our unpublished data).

Various Mechanisms May Lead from Inhibition of HSP90 to Cleavage of ErbB2

The interaction between HSP90 and its clients occurs in a repetitive ATP-dependent manner, which includes temporary association to several cochaperones and is often termed the chaperone cycle (Caplan *et al.*, 2007). If the chaperone cycle is inhibited, e.g., by GA, then the cochaperone and ubiquitin ligase carboxyl terminus of HSP70-interacting protein (CHIP) is recruited to the ErbB2-associated chaperone complex stimulating ubiquitinylation of ErbB2 (Xu *et al.*, 2002; Zhou *et al.*, 2003; Whitesell and Lindquist, 2005; Caplan *et al.*, 2007). Overexpression of CHIP stimulates ErbB2 ubiquitinylation and degradation, whereas overexpression of a ligase-inactive version of CHIP inhibits ErbB2 ubiquitinylation. However, ErbB2 degradation after HSP90 inhibition is not completely abolished in CHIP−/− mouse embryonic fibroblasts (Xu *et al.*, 2002; Zhou *et al.*, 2003). We speculate that overexpression of ligase-inactive CHIP would inhibit GA-induced ErbB2 C-terminal cleavage and subsequent internalization. It would be relevant for future studies to address this, as well as if overexpression of CHIP itself could induce ErbB2 C-terminal cleavage and internalization.

Tikhomirov and Carpenter (2000) tested a range of protease inhibitors in order to characterize the protease(s) responsible for ErbB2 C-terminal cleavage and found that cleavage was inhibited most efficiently by ALLN, less efficiently by lactacystin, and to some extent by the cathepsin B inhibitor Ca074Me. Concordantly, we observed similar effects by these inhibitors on cleavage of YEC (Figure 7, B and C and our unpublished data). ALLN is known to inhibit a range of proteases, most notably the proteasome and calpains; however calpains are not responsible for the cleavage of ErbB2 (Tikhomirov and Carpenter, 2000). If the proteasome is the actual protease cleaving ErbB2 as hypothesized above, it is puzzling why cleavage can be inhibited with the cathepsin inhibitor Ca074Me, except if it has so far unreported off target effects. An alternative explanation involves

lysosomal rupture that has been shown to precede and cause apoptosis (Guicciardi *et al.*, 2004; Fehrenbacher and Jaattela, 2005), and it remains a possibility that GA induces a proteasome-dependent lysosome destabilization releasing varying amounts of cathepsins to the cytosol.

The C-Terminus of ErbB2 May Inhibit ErbB2 Internalization

It has been suggested that the resistance of ErbB2 toward endocytosis is due to a retention mechanism (Sorkin *et al.*, 1993; Austin *et al.*, 2004; Hommelgaard *et al.*, 2004; Lerdrup *et al.*, 2006), and a single study suggested that this is mediated through the C-terminal tail of ErbB2 (Sorkin *et al.*, 1993). We here show that the C-terminally cleaved ErbB2 is internalized far more readily than full-length ErbB2, supporting that the C-terminus of ErbB2 inhibits its internalization as previously proposed (Sorkin *et al.*, 1993). There are essentially two different interpretations of this phenomenon: 1) a cryptic motif that stimulates endocytosis is normally hidden and becomes exposed when the C-terminal part of ErbB2 is lacking. 2) Alternatively, full-length ErbB2 could be retained from the endocytic machinery by one of several possible means. The retention could be due to a stable protein–protein association, a dynamic but frequent protein-protein association, a factor competing with endocytic proteins for ErbB2 binding, or removal of covalent modifications recruiting endocytic proteins, e.g., by a deubiquitinase. Future research should address which of the putative mechanisms are responsible for retaining ErbB2 from the endocytic machinery. Given the clear link between ErbB2 overexpression and cancers it is highly important to improve our understanding of this mechanism and identify its components.

ACKNOWLEDGMENTS

We appreciate the skilled technical assistance offered by Ulla Hjortenberg, Mette Ohlsen, and Izabela Rasmussen. This study was supported by grants from the Danish Cancer Society, the Danish Cancer Research Foundation, the Danish Medical Research Council, the Novo Nordic Foundation, and the John and Birthe Meyer Foundation.

REFERENCES

Austin, C. D., De Maziere, A. M., Pisacane, P. I., van Dijk, S. M., Eigenbrot, C., Sliwkowski, M. X., Klumperman, J., and Scheller, R. H. (2004). Endocytosis and sorting of ErbB2 and the site of action of cancer therapeutics trastuzumab and geldanamycin. Mol. Biol. Cell *15*, 5268–5282.

Baulida, J., Kraus, M. H., Alimandi, M., Di Fiore, P. P., and Carpenter, G. (1996). All ErbB receptors other than the epidermal growth factor receptor are endocytosis impaired. J. Biol. Chem. *271*, 5251–5257.

Bendtsen, J. D., Nielsen, H., von, H. G., and Brunak, S. (2004). Improved prediction of signal peptides: SignalP 3.0. J. Mol. Biol. *340*, 783–795.

Bucci, C., Thomsen, P., Nicoziani, P., McCarthy, J., and van Deurs, B. (2000). Rab7, a key to lysosome biogenesis. Mol. Biol. Cell *11*, 467–480.

Burack, M. A., Silverman, M. A., and Banker, G. (2000). The role of selective transport in neuronal protein sorting. Neuron *26*, 465–472.

Caplan, A. J., Mandal, A. K., and Theodoraki, M. A. (2007). Molecular chaperones and protein kinase quality control. Trends Cell Biol. *17*, 87–92.

Citri, A., Alroy, I., Lavi, S., Rubin, C., Xu, W., Grammatikakis, N., Patterson, C., Neckers, L., Fry, D. W., and Yarden, Y. (2002). Drug-induced ubiquitylation and degradation of ErbB receptor tyrosine kinases: implications for cancer therapy. EMBO J. *21*, 2407–2417.

De Placido, S., Carlomagno, C., De Laurentiis, M., and Bianco, A. R. (1998). c-erbB2 expression predicts tamoxifen efficacy in breast cancer patients. Breast Cancer Res. Treat. *52*, 55–64.

Fehrenbacher, N. and Jaattela, M. (2005). Lysosomes as targets for cancer therapy. Cancer Res. *65*, 2993–2995.

Guicciardi, M. E., Leist, M., and Gores, G. J. (2004). Lysosomes in cell death. Oncogene *23*, 2881–2890.

Gupta-Rossi, N., Six, E., LeBail, O., Logeat, F., Chastagner, P., Olry, A., Israel, A., and Brou, C. (2004). Monoubiquitination and endocytosis direct gamma-secretase cleavage of activated Notch receptor. J. Cell Biol. *166*, 73–83.

Haass, C. and De, S. B. (1999). The presenilins in Alzheimer's disease—proteolysis holds the key. Science *286*, 916–919.

Haslekas, C., Breen, K., Pedersen, K. W., Johannessen, L. E., Stang, E., and Madshus, I. H. (2005). The inhibitory effect of ErbB2 on epidermal growth factor-induced formation of clathrin-coated pits correlates with retention of epidermal growth factor receptor-ErbB2 oligomeric complexes at the plasma membrane. Mol. Biol. Cell *16*, 5832–5842.

He, Y. Y., Huang, J. L., and Chignell, C. F. (2006). Cleavage of epidermal growth factor receptor by caspase during apoptosis is independent of its internalization. Oncogene *25*, 1521–1531.

Hommelgaard, A. M., Lerdrup, M., and van Deurs, B. (2004). Association with membrane protrusions makes ErbB2 an internalization-resistant receptor. Mol. Biol. Cell *15*, 1557–1567.

Hong, R. L., Spohn, W. H., and Hung, M. C. (1999). Curcumin inhibits tyrosine kinase activity of p185neu and also depletes p185neu. Clin. Cancer Res. *5*, 1884–1891.

Hynes, N. E. and Stern, D. F. (1994). The biology of erbB-2/neu/HER-2 and its role in cancer. Biochim. Biophys. Acta *1198*, 165–184.

Klapper, L. N., Kirschbaum, M. H., Sela, M., and Yarden, Y. (2000). Biochemical and clinical implications of the ErbB/HER signaling network of growth factor receptors. Adv. Cancer Res. *77*, 25–79.

Lerdrup, M., Hommelgaard, A. M., Grandal, M., and van Deurs, B. (2006). Geldanamycin stimulates internalization of ErbB2 in a proteasome-dependent way. J. Cell Sci. *119*, 85–95.

Longva, K. E., Pedersen, N. M., Haslekas, C., Stang, E., and Madshus, I. H. (2005). Herceptin-induced inhibition of ErbB2 signaling involves reduced phosphorylation of Akt but not endocytic down-regulation of ErbB2. Int. J. Cancer *116*, 359–367.

Magnifico, A., Albano, L., Campaner, S., Campiglio, M., Pilotti, S., Menard, S., and Tagliabue, E. (2007). Protein kinase Cα determines HER2 fate in breast carcinoma cells with HER2 protein overexpression without gene amplification. Cancer Res. *67*, 5308–5317.

Mimnaugh, E. G., Chavany, C., and Neckers, L. (1996). Polyubiquitination and proteasomal degradation of the p185c-erbB-2 receptor protein-tyrosine kinase induced by geldanamycin. J. Biol. Chem. *271*, 22796–22801.

Moorthy, A. K., Savinova, O. V., Ho, J. Q., Wang, V. Y., Vu, D., and Ghosh, G. (2006). The 20S proteasome processes NF-kappaB1 p105 into p50 in a translation-independent manner. EMBO J. *25*, 1945–1956.

Muthuswamy, S. K., Gilman, M., and Brugge, J. S. (1999). Controlled dimerization of ErbB receptors provides evidence for differential signaling by homo and heterodimers. Mol. Cell. Biol. *19*, 6845–6857.

Ni, C. Y., Murphy, M. P., Golde, T. E., and Carpenter, G. (2001). gamma-secretase cleavage and nuclear localization of ErbB-4 receptor tyrosine kinase. Science *294*, 2179–2181.

Pegram, M. D., Pauletti, G., and Slamon, D. J. (1998). HER-2/neu as a predictive marker of response to breast cancer therapy. Breast Cancer Res. Treat. *52*, 65–77.

Petrelli, A., Circosta, P., Granziero, L., Mazzone, M., Pisacane, A., Fenoglio, S., Comoglio, P. M., and Giordano, S. (2006). Ab-induced ectodomain shedding mediates hepatocyte growth factor receptor down-regulation and hampers biological activity. Proc. Natl. Acad. Sci. USA *103*, 5090–5095.

Selkoe, D. J., Yamazaki, T., Citron, M., Podlisny, M. B., Koo, E. H., Teplow, D. B., and Haass, C. (1996). The role of APP processing and trafficking pathways in the formation of amyloid beta-protein. Ann. NY Acad. Sci. *777*, 57–64.

Shimizu, H., Seiki, T., Asada, M., Yoshimatsu, K., and Koyama, N. (2003). Alpha6beta1 integrin induces proteasome-mediated cleavage of erbB2 in breast cancer cells. Oncogene *22*, 831–839.

Slamon, D. J., Clark, G. M., Wong, S. G., Levin, W. J., Ullrich, A., and McGuire, W. L. (1987). Human breast cancer: correlation of relapse and survival with amplification of the HER-2/neu oncogene. Science *235*, 177–182.

Sorkin, A., Di Fiore, P. P., and Carpenter, G. (1993). The carboxyl terminus of epidermal growth factor receptor/erbB-2 chimerae is internalization impaired. Oncogene *8*, 3021–3028.

Sugahara, K. N., Hirata, T., Hayasaka, H., Stern, R., Murai, T., and Miyasaka, M. (2006). Tumor cells enhance their own CD44 cleavage and motility by generating hyaluronan fragments. J. Biol. Chem. *281*, 5861–5868.

Tikhomirov, O., and Carpenter, G. (2000). Geldanamycin induces ErbB-2 degradation by proteolytic fragmentation. J. Biol. Chem. *275*, 26625–26631.

Tikhomirov, O., and Carpenter, G. (2001). Caspase-dependent cleavage of ErbB-2 by geldanamycin and staurosporin. J. Biol. Chem. *276*, 33675–33680.

Tikhomirov, O., and Carpenter, G. (2003). Identification of ErbB-2 kinase domain motifs required for geldanamycin-induced degradation. Cancer Res. *63*, 39–43.

van Deurs, B., Holm, P. K., and Sandvig, K. (1996). Inhibition of the vacuolar H(+)-ATPase with bafilomycin reduces delivery of internalized molecules from mature multivesicular endosomes to lysosomes in HEp-2 cells. Eur. J. Cell Biol. *69*, 343–350.

Vernimmen, D., Gueders, M., Pisvin, S., Delvenne, P., and Winkler, R. (2003). Different mechanisms are implicated in ERBB2 gene overexpression in breast and in other cancers. Br. J. Cancer *89*, 899–906.

Wallenius, V., Hisaoka, M., Helou, K., Levan, G., Mandahl, N., Meis-Kindblom, J. M., Kindblom, L. G., and Jansson, J. O. (2000). Overexpression of the hepatocyte growth factor (HGF) receptor (Met) and presence of a truncated and activated intracellular HGF receptor fragment in locally aggressive/malignant human musculoskeletal tumors. Am. J. Pathol. *156*, 821–829.

Wang, Z., Zhang, L., Yeung, T. K., and Chen, X. (1999). Endocytosis deficiency of epidermal growth factor (EGF) receptor-ErbB2 heterodimers in response to EGF stimulation. Mol. Biol. Cell *10*, 1621–1636.

Way, T. D., Kao, M. C., and Lin, J. K. (2004). Apigenin induces apoptosis through proteasomal degradation of HER2/neu in HER2/neu-overexpressing breast cancer cells via the phosphatidylinositol 3-kinase/Akt-dependent pathway. J. Biol. Chem. *279*, 4479–4489.

Whitesell, L. and Lindquist, S. L. (2005). HSP90 and the chaperoning of cancer. Nat. Rev. Cancer *5*, 761–772.

Wiley, H. S. and Burke, P. M. (2001). Regulation of receptor tyrosine kinase signaling by endocytic trafficking. Traffic. *2*, 12–18.

Worthylake, R., Opresko, L. K., and Wiley, H. S. (1999). ErbB-2 amplification inhibits down-regulation and induces constitutive activation of both ErbB-2 and epidermal growth factor receptors. J. Biol. Chem. *274*, 8865–8874.

Xu, W., Marcu, M., Yuan, X., Mimnaugh, E., Patterson, C., and Neckers, L. (2002). Chaperone-dependent E3 ubiquitin ligase CHIP mediates a degradative pathway for c-ErbB2/Neu. Proc. Natl. Acad. Sci. USA *99*, 12847–12852.

Xu, W., Mimnaugh, E., Rosser, M. F., Nicchitta, C., Marcu, M., Yarden, Y., and Neckers, L. (2001). Sensitivity of mature Erbb2 to geldanamycin is conferred by its kinase domain and is mediated by the chaperone protein Hsp90. J. Biol. Chem. *276*, 3702–3708.

Yarden, Y. (2001). Biology of HER2 and its importance in breast cancer. Oncology *61*(Suppl 2), 1–13.

Zampieri, N., Xu, C. F., Neubert, T. A., and Chao, M. V. (2005). Cleavage of p75 neurotrophin receptor by alpha-secretase and gamma-secretase requires specific receptor domains. J. Biol. Chem. *280*, 14563–14571.

Zheng, F. F., Kuduk, S. D., Chiosis, G., Munster, P. N., SeppLorenzino, L., Danishefsky, S. J., and Rosen, N. (2000). Identification of a geldanamycin dimer that induces the selective degradation of HER-family tyrosine kinases. Cancer Res. *60*, 2090–2094.

Zhou, P., Fernandes, N., Dodge, I. L., Reddi, A. L., Rao, N., Safran, H., DiPetrillo, T. A., Wazer, D. E., Band, V., and Band, H. (2003). ErbB2 degradation mediated by the co-chaperone protein CHIP. J. Biol. Chem. *278*, 13829–13837.